Journal of Proteomics & Bioinformatics - Open Access

Research Article JPB/Vol.2/June 2009

Epac-induced Alterations in the Proteome of Human SH-SY5Y Neuroblastoma Cells

Even Birkeland[1,2], Gyrid Nygaard[1,2], Eystein Oveland[2], Olav Mjaavatten[1,2], Marie Ljones[1], Stein Ove Doskeland[2], Camilla Krakstad[2] and Frode Selheim[1,2*]

[1]Proteomic Unit at University of Bergen, Bergen, Norway
[2]Department of Biomedicine, University of Bergen, Bergen, Norway

*Corresponding author: Frode Selheim, Department of Biomedicine, University of Bergen, Jonas Lies vei 91, N-5009 Bergen, Norway, Tel: +47 55 586091; Fax: +47 5 5586360; E-mail: frode.selheim@biomed.uib.no

Received April 27, 2009; Accepted June 06, 2009; Published June 08, 2009

Citation: Birkeland E, Nygaard G, Oveland E, Mjaavatten O, Ljones M, et al. (2009) Epac-induced Alterations in the Proteome of Human SH-SY5Y Neuroblastoma Cells. J Proteomics Bioinform 2: 244-254. doi:10.4172/jpb.1000083

Abstract

The hitherto proteome of the human neuroblastoma cell line SH-SY5Y consists of 1029 unique proteins. By using subcellular fractionation, SDS PAGE and nanoLC-Q-TOF-MS/MS we enlarged the proteome with additionally 72.2%, resulting in 3707 unique proteins.

The stage of neuroblastoma tumor cell differentiation is known to influence patient outcome, with a high differentiation stage correlating to favourable prognosis. To elucidate the effects of cAMP in SH-SY5Y neuroblastoma differentiation we used selective cAMP analogs to activate Epac and PKA.

We found that activation of Epac induced actin and tubulin polymerization and neurite outgrowth, whereas PKA activation did not. The effects of the Epac stimulation were abolished by knock down of Epac1 with ShRNA.

Stable isotope labelling with amino acids in cell culture (SILAC) and mass spectrometry were used to disclose the long-time effects of Epac activation on the SH-SY5Y proteome. We found 101 expressed proteins upregulated and 74 downregulated. Upregulated proteins were in general associated with neuronal cell differentiation and adhesion, whereas downregulated proteins typically were involved in RNA processing. We conclude that cAMP-induced morphological and biochemical neuronal differentiation of human neuroblastoma SH-SY5Y cells are mediated by Epac.

Keywords: Proteomics; Neuroblastoma; Epac; Differentiation; SILAC; LC-MS/MS

Introduction

The SH-SY5Y cell line is a subclone of the human neuroblastoma cell line SK-N-SH originally established from the bone marrow (Biedler et al., 1973; Ross et al., 1983). Neuroblastoma cells are typically arrested at an early and immature stage. Despite this the SH-SY5Y cell line is capable of undergoing neuronal differentiation when exposed to the proper growth conditions (Pahlman et al., 1995). The cell line also contains mutations in the anaplastic lymphoma kinase (ALK), which is the main cause of familial neuroblastoma (Chen et al., 2008; George et al., 2008; Janoueix-Lerosey et al., 2008; Mosse et al., 2008). These characteristics together with a distinct sensitivity to oxidative stress makes the neuroblastoma SH-SY5Y cell line an excellent model system to study neuronal differentiation and neuroblastoma tumourigenesis, as well as several aspects of neuronal degenerative diseases (Schaeffer et al., 2008). Unravelling the proteome of this cell line is of great importance to support such studies.

Gilany et al. have previously analyzed the proteome of the SH-SY5Y cell line, identifying 1103 proteins. By using ProteinCenter software to removes redundancy, we observed that the formerly SH-SY5Y proteome (1103 proteins) contained 74 entries/accession keys which pointed to the same protein. By using both total cell lysates and subcellular fractionation, SDS PAGE and LC-Q-TOF-MS/MS we here expand the previously reported proteome of the SH-SY5Y cell line (Gilany et al., 2008).

The pituitary adenylate cyclase activating peptide (PACAP) has recently been reported to induce neuronal differentiation of SH-SY5Y cells through a cAMP-dependent protein kinase (PKA)-independent mechanism (Monaghan et al., 2008). With the exception of cyclic nucleotide gated (CNG) cation channels, the cAMP mediated signalling was initially attributed solely to the activation of PKA (Zufall et al., 1997). When the exchange protein directly activated by cAMP (Epac) was discovered in 1998 more complexity was added to cAMP-mediated signalling (de Rooij et al., 2000; de Rooij et al., 1998; Kawasaki et al., 1998). To this date, two isoforms of Epac, Epac1 and Epac2, have been identified. Epac1 and Epac2 are guanine nucleotide exchange factors (GEFs) for the small GTPases Rap1 and Rap2 (Bos, 2006). The development of cAMP analogs specific for Epac and PKA enabled further functional characterization, and as a result several other effector proteins of Epac have been identified (Christensen et al., 2003; Holz et al., 2008). Both PKA and Epac have been implicated in the process of neuronal differentiation (Shi et al., 2006). In vivo studies have shown that the stage of neuronal tumour cell differentiation influences patient outcome, with a high differentiation stage correlating to favourable prognosis (Edsjo et al., 2007; Hedborg et al., 1995).

Our group has previously reported that the cAMP effectors Epac and PKA promote neurite extension in PC-12 rat pheochromocytoma cells (Christensen et al., 2003).

In this study we investigated the effect of the Epac specific cAMP analog 8-pCPT-2'-O-Me-cAMP and the PKA specific cAMP analog N^6-Benzoyl-cAMP in SH-SY5Y wild type and SH-SY5Y Epac1 knock down cells. Intriguingly, we identified Epac1, and not PKA, as an inducer of cytoskeleton polymerization and neurite outgrowth. As a result of this, we applied a quantitative proteomics study using stable isotope labelling with amino acids in cell culture (SILAC) on SH-SY5Y cells in the presence or absence of 8-pCPT-2'-O-Me-cAMP for 16 hours. Here we present evidence showing that Epac activation induces alteration of protein expression that favours differentiation of human SH-SY5Y cells towards a sympathetic neuronal phenotype.

Materials and Methods

Cell Culture

The SH-SY5Y (ATTCC no: CRL-2266) human neuroblastoma cell line was cultured as monolayer cells in Dulbeccos Modified Eagles Medium (DMEM) enriched with 10% foetal calf serum (FCS) (Invitrogen, Carlsbad, CA) and 1% penicillin-streptomycin. The cells were grown at 37 ºC in a humidified 5 % CO_2,95 % air incubator. At 80 % confluence cells were detached in PBS by mild flushing, and re-seeded at 25% confluence in 10% conditioned DMEM.

For metabolic labelling cells were grown in L-lysine, L-arginine and L-glutamine deficient DMEM (Invitrogen, Carlsbad, CA) with 10 % dialysed FCS and supplemented with "light" $^{12}C_6$ L-lysine (0.8 mM) and $^{12}C_6$ L-arginine (0.2 mM), or the same concentration of "heavy" $^{13}C_6$ marked isotopes. The cells were cultured in a reduced amount of arginine compared to standard DMEM, to avoid $^{13}C_6$-arginine to $^{13}C_5$-proline conversion. SH-SY5Y cells reaching 80-90 % confluence was split 1:2 and added fresh medium with 10 % dialysed FCS and L-glutamine (2mM).

After six generations, cells metabolically labelled with $^{13}C_6$ L-arginine- and $^{13}C_6$ L-lysine were stimulated for 16 hours with the selective Epac activator 8-pCPT-2'-O-Me-cAMP (250 µM, BIOLOG Life Science Institute, Germany).

Transfection

SH-SY5Y cells were transfected using Sure Silencing shRNA Plasmid Kit from Super Array (SA Biosciences, MD, USA). The Sure Silencing™ shRNA Plasmids are designed to specifically knock down the expression of individual genes by RNA interference under transient transfection. The vector contains the shRNA under control of the U1 promoter and the GFP gene, while the control vector contains GFP only. Transfection was carried out according to the manufacturer's instructions. SH-SY5Y (100 000 cells/ml) cells were seeded in normal growth medium in a 24 well Nunc plate, prior to transfection. The total concentration of plasmid used in each well was 6 ng/ml. Lipofectamine 2000 was mixed with serum-free DMEM medium in a 1:25 ratio, and the plasmid was mixed in a ratio of 1:50 with serum-free medium. The plasmid-lipofectamine solution was carefully applied to the cells, followed by gentle shaking of the plate. Transfected SH-SY5Y cells were treated with 250 µM 8-pCPT-2´-O-Me-cAMP for 16 hours. Pictures were taken at 20x magnification using a Zeiss Axiovert 200M Imaging microscope (Carl Zeiss MicroImaging GMbH, Germany).

Cell lysis and Subcellular Fractionation

The cells were washed twice in cold PBS before lysis in 10 mM K_2HPO_4, 10 mM KH_2PO_4, 1 mM EDTA (pH 6.8), 10 mM CHAPS, 50 µM NaF, 0.3 µM $NaVO_3$ supplemented with Complete mini protease inhibitor (Roche Molecular Biochemical, Basel, Switzerland). Cell debris was removed by centrifugation at 17,500 g for 10 min at 4ºC. For subcellular fractionation, the cells were treated according to the protocol for Qproteome Cell Compartment Kit from Qiagen (Qiagen, Hilden, Germany) resulting in separate cytosol, membrane, nucleus, and cytoskeleton fractions.

Protein Separation

The protein concentration of the cell lysates were determined using the standard Bradford method (Bradford, 1976). To identify and quantify proteins expressed in the neuroblastoma SH-SY5Y cell line, the fractionated cell lysates, or total lysates from heavy $^{13}C_6$ marked (stimulated) and light $^{12}C_6$ marked (control) cells, were separated on a 5-15 % SDS-PAGE gradient gel (20cm long). The gels were stained with Coomassie Brilliant Blue (0.1 % Coomassie Brilliant Blue, 50 % methanol, 10 % acetic acid) and sliced crosswise into 35-40 bands for each lane. The gel pieces were in-gel trypsinated as previously described by Shevchenco et al. (Shevchenko et al., 2006), and recovered tryptic peptides were applied to nanoflow LC-Q-TOF-MS/MS for automated data dependent acquisition (for achieved MS data see Appendix 1 and 2). In order to avoid matches to the same protein from different entries the identified proteins were merged with >85% sequence homology using ProteinCenter software version 2.7 (Proxeon Bioinformatics, Odense, Denmark).

Mass Spectrometry Analysis

Mass spectrometry analysis was performed essentially as recently described (Oveland et al., 2009). Briefly, the $^{12}C_6$/$^{13}C_6$ peptide samples were injected into a nanoflow HPLC-system (UltiMate 3000 from Dionex Corporation, CA, USA) on-line with positive electrospray ionization on a Quadropole-Time of Flight Ultima Global instrument (Q-TOF) (Waters, Micromass, Manchester, UK). Samples were desalted on a precolumn cartridge (C_{18} Pepmap 100 from Dionex, 5 µm particle size, 100Å pore size, 300 µm i.d. x 5 mm) for 4 minutes (isocratic flow rate of 25 µl aqueous 2% ACN in 0.05% TFA/min) before separation on the analytical column (Reprosil-Pur 5 µm, 120Å C_{18} resin Dr. Maisch Gmbh, Germany packed in-house in a 15cm x 75µm ID fused silica capillary). The peptides were eluted from the column during a mobile phase gradient (solvent A: aqueous 2% ACN in 0.1% FA, solvent B: aqueous 90% ACN in 0.1% FA) as follows: Solvent B was increased rapidly from 5 to 12% (0 - 2 minutes), followed by a slow increase from 12 to 30% (2 – 50 minutes) and from 30 to 50% (50 – 73 minutes). The majority of peptides was then eluted from the column at a constant flow rate of 300 nl/min. Elution of very hydrophobic peptides and conditioning of the column, were performed during 10 minutes isocratic elution with 95% solvent B and 15 minutes isocratic elution with 5% B, respectively. The eluting peptides were ionized in the electrospray and analyzed by the Q-TOF. The Q-TOF was operated in Data Directed Aquisition mode using a 1second MS survey scan. CID spectrum acquisition was allowed for up to a total of 2 seconds on each precursor ion or stopped when the signal intensity fell below ten counts per second respectively before a new MS to MS/MS cycle was started. Precursors were excluded from MS/MS experiments for one minute and singly charged ions were excluded as precursors for MS/MS.

The LC-Q-TOF/MS and MS/MS generated raw data spectra were analyzed using the software Virtual Expert Mass Spectrometrist (VEMS) version 3.3 (Matthiesen et al., 2005). The spectra were matched to predicted precursor ions and fragmentation patterns in the human International Protein Index (IPI) database version 3.3.2 (Kersey et al., 2004). VEMS default-settings were used for both identification and quantification. The algorithms for scoring and identification using VEMS have been explained in detail by Matthiesen et al. (Matthiesen et al., 2004; Matthiesen et al., 2005). In brief, the enzyme specific settings were trypsin cleavage C-terminal to arginine and lysine with one missed cleavage allowed. In the method specific settings, carbamidomethylation (CAM) of cysteine was set as a fixed modification and methionine oxidation (M_oxidation), $^{13}C_6$-L-arginine (R_6 x 13C) and $^{13}C_6$-L-lysine (K_6 x 13C) were added as variable modifications for the whole database. The molecular mass accuracy of precursor and fragment peptides was set to +/- 500 mDa for identification. The score threshold for accepting individual spectra was set to 10. The false discovery rate (FDR) was calculated as the number of matches in a reversed IPI database (false positives) divided by the sum of proteins identified (number of matches in the IPI and the IPI reversed combined). The reversed database was generated by using the software Scaffold version 2.1.0. (Proteome Software Inc. Portland, OR, USA). The FDRs were below 2% in all data sets (FDR: cytosol fraction 1,6; membrane fraction 0,9; nucleus fraction 1,6; cytoskeleton fraction 1,3; total lysates 1,9; lysates for quantification 0,4).

For quantification, we used VEMS default-settings and performed the data analysis as recently explained in detail

by Lund et al. (Lund et al., 2009). Briefly, the molecular mass accuracy was set to +/- 100 mDa. The VEMS software was set to quantify the first 3 peptide isotopes (light (L) isotopic set of peaks versus heavy (H) isotopic set of peaks), and the cutoff score of the peptides was set to 20, with 5 as the maximum standard deviation. The relative abundance ratio for differentially expressed proteins was calculated from the spectral intensities of heavy peaks divided by the sum of heavy and light peaks (H/H+L). Thus, a relative ratio of 0.5 or 50% means equal quantities of expressed proteins for the compared samples.

ProteinCenter and the open-source bioinformatics database DAVID (Dennis et al., 2003; Hosack et al., 2003) were used to analyze the protein data.

Based on the average quantitative ratio mean, a quantification value-dependent normalization function (*f(x)*) was calculated according to the equations described by Lund et al. (Lund et al., 2009). See Appendix 1 for details about accession keys, gene ontology (GO)-slim terms, PFAMS, the quantification value-dependent normalization function, normalized quantification values, number of peptides, scores, standard deviation and number of unique peptide sequences for regulated proteins. See Appendix 2 for information about all identified and quantified peptides, the sequence coverage, precursor m/z observed and precursor charge observed.

Confocal Microscopy

SH-SY5Y cells (100 000 cells/ml) were seeded onto 15 mm round glass cover slips (Assistant, Germany) the day before the experiment. Cells were treated without (control) or with 0.25 mM of the Epac agonist 8-pCPT-2´-O-Me-cAMP and/or 0.2 mM of the PKA agonist N^6-Benzoyl-cAMP (BIOLOG Life Science Institute, Germany) agonist for 16 hours. Cells were fixed in 2% formaldehyde for 1 hour in room temperature (RT). After two washes in washing buffer (WB: PBS, 1mg/ml BSA, 0.2% Na-azid) cells were permeabilised using 0.1% Triton X-100 in PBS for 20 minutes at 4°C. The cells were washed in WB prior to reducing non-specific binding of the antibody by blocking in 1 mg/ml BSA with 0,5% NP-40 in PBS for one hour. Tubulin staining was performed by incubation for 30 minutes with primary antibody (mouse anti-β-tubulin) in RT, followed by washing in WB, and incubation with secondary antibody (goat-anti-mouse IgG-FITC), for three hours in RT. Tubulin staining was followed by washing, and a direct staining of actin by 30 minutes incubation with fluorescein-conjugated phalloidin (F432, Molecular probes, Netherlands). Finally, the cover slips were mounted in Vectashield (Vector Laboratories, Burlingame, CA). Imaging was performed using the Zeiss LSM 510 META (Carl Zeiss MicroImaging GMbH, Germany) confocal laser microscope. The samples were examined with a 40x1.3 NA Plan-Neofluor oil-immersion objective. Fluorescent images were acquired with Argon/Helium Neon (Zeiss) lasers and processed using Adobe Photoshop CS software (Adobe Systems, San Jose, CA, USA).

Results and Discussion

The Enlargement of the Human SH-SY5Y Proteome

Using both total cell lysates and subcellular fractionation in combinations with SDS PAGE and LC-Q-TOF-MS/MS

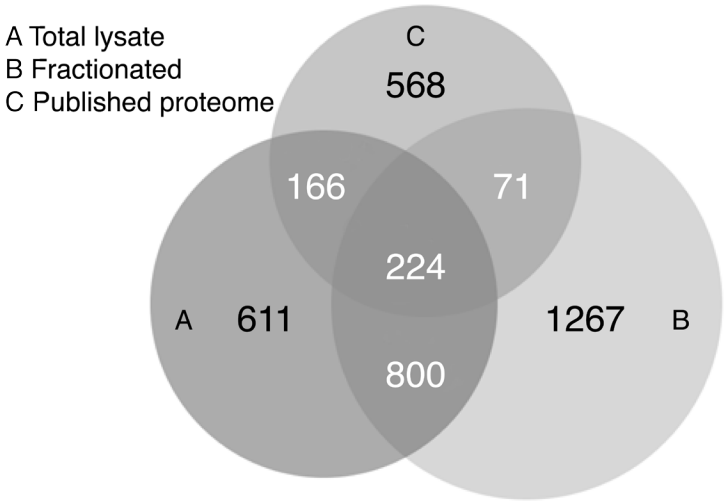

Set	Count	%
A	1801	48.6
B	2362	63.7
C	1029	27.8
A ∪ B - C	2678	72.2
A ∩ B - C	800	21.6
A ∩ B ∩ C	224	6.0
A ∪ B ∪ C	3707	100.0

Figure 1: The human SH-SY5Y proteome
The figure shows Venn diagram of unique identified proteins from total cell lysates (A) and subcellular fractionation (B), as well as the resemblance between formerly identified proteins (C) and our identified proteins in SH-SY5Y neuroblastoma cells**.** By using ProteinCenter software to remove redundancy, we observed that the formerly SH-SY5Y proteome (1103 proteins (Gilany et al., 2008)) contained 74 entries/accession keys which pointed to the same protein. The former SH-SY5Y proteome, here presented as 1029 proteins, is hereby extended by additionally 2678 unique proteins resulting in 3707 unique proteins.

we were able to expand the previously reported neuroblastoma cell line SH-SY5Y proteome (1029 single hit proteins) (Gilany et al., 2008) with additionally 72.2 % (2678 unique proteins with 2 or more identified peptides) resulting in 3707 unique proteins (Figure 1 and Appendix 1 and 2). Comparing our proteomic data with that of the recently published data of the SH-SY5Y proteome (Gilany et al., 2008), we found only 6 % overlap (224 proteins) in unique identified proteins between the datasets (Figure 1). In our gene ontology analysis we used the DAVID program package. We merged our datasets, five in total (see Appendix 1), to unveil the properties of the SH-SY5Y proteome.

We used DAVID to group and annotate proteins into the GO cellular component (CC:3) and GO molecular function (MF:3) terms, a remarkable similarity in enriched terms was found for our datasets (Appendix 1) and the recently published data (Gilany et al., 2008). However, intracellular part (79.3%), intracellular organelle (66.3%) and cytoplasm (58.2%) were highly enriched in our dataset.

The most significantly enriched GO term, in relative to the "theoretical human proteome" for molecular function includes; intracellular part (P-value 3.40E-209), and cytoplasmic proteins (P-value 1.70E-156), RNA binding (P-value 5.40E-74), hydrolase activity (P-value 1.20E-42) and purine nucleotide binding (P-value 4.10E-34). For analysis of the fractionated data see Appendix 1.

The Epac-activating cAMP Analog 8-pCPT-2´-O-Me-cAMP Promotes Neurite Extension in SH-SY5Y Cells

The pituitary adenylate cyclase activating peptide has recently been reported to induce neuronal differentiation of SH-SY5Y cells through a PKA-independent mechanism (Monaghan et al., 2008). To investigate the effect of Epac on Human SH-SY5Y neuroblastoma cells we used analogs of cAMP, which is selective for Epac (8-pCPT-2´-O-Me-cAMP, 250 µM) and PKA (N^6-Benzoyl-cAMP, 200 µM) (Christensen et al., 2003). As shown in Figure 2, 8-pCPT-2´-O-Me-cAMP induced long neurite extensions and the soma was wider and more attached to the substrate than the control cells. Immunofluorescent staining showed reorganisation and enrichment of actin and tubulin in neurites. An increase in focal points (small actin rich dots)

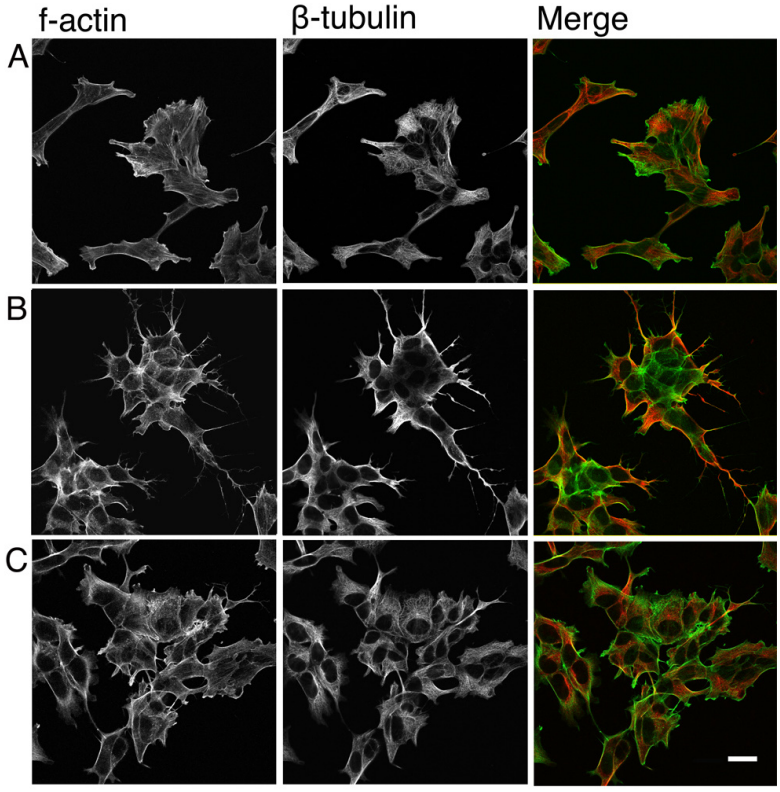

Figure 2: Epac-induced actin and tubulin polymerization in SH-SY5Y cells
The micrographs show unstimulated (A) and stimulated human SH-SY5Y cells for 16 hours with (B) Epac agonist (250 µM, 8-pCPT-2´-O-Me-cAMP) or with (C) PKA agonist (200 µM, N^6-benzoyl-cAMP). Tubulin was stained with primary β-tubulin mouse monoclonal antibody, secondary antibody (goat-anti-mouse IgG-TRITC, red), actin was stained with fluorescein-conjugated phalloidine (green). The data shown is representative of three independent experiments. Bar=20 µm.

could also be observed in the Epac-selective cAMP analog treated cells. In contrast, neurite elongation and large reorganisation of cytoskeleton were not observed in SH-SY5Y cells stimulated with the selective PKA activator N^6-Benzoyl-cAMP. Moreover, we observed reduced proliferation and a slightly increase in apoptosis for Epac-stimulated differentiating SH-SY5Y cells, whereas selective PKA activation led to increased proliferation. Interestingly, as previously shown by others for PC12 cells (Kiermayer et al., 2005), the proliferative PKA induced signalling was reversed into an anti-proliferative and differentiating response in the company of selective Epac activation (data not shown).

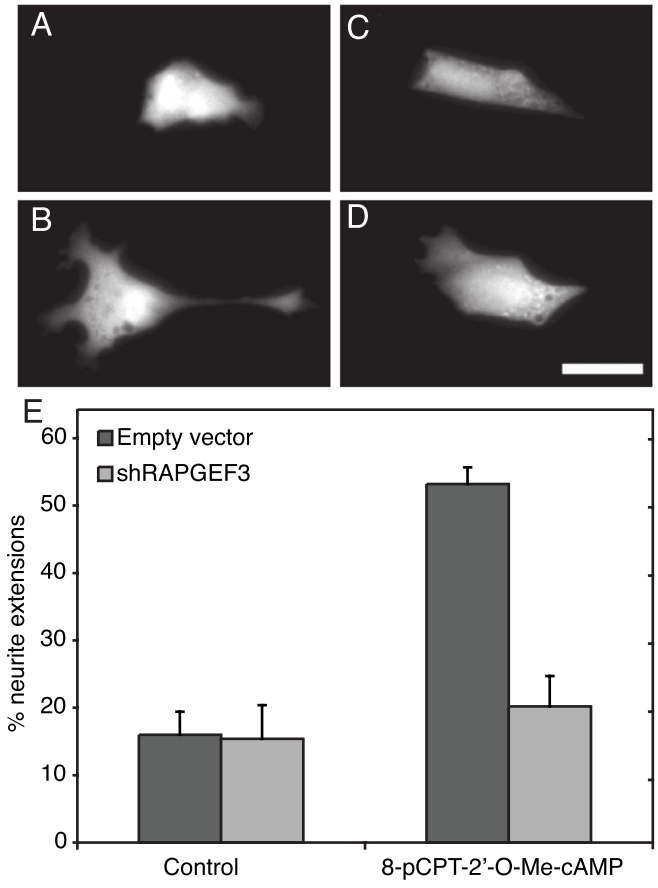

Figure 3: cAMP induced neurite extensions in SH-SY5Y neuroblastoma cells are mediated by Epac

Transfected SH-SY5Y cells were treated with 250 µM 8-pCPT-2´-O-Me-cAMP, for 16 hours. The percentage of neurite extensions was determined by counting cells with neurite extensions > 10 µm. Figure A, B, C and D shows the morphological features of transfected SH-SY5Y cells: (A) SH-SY5Y cells transfected with empty vector (control), (B) SH-SY5Y cells transfected with empty vector and treated with Epac agonist, (C) SH-SY5Y cells transfected with shRAPGEF3, and (D) SH-SY5Y cells transfected with shRAPGEF3 and treated with Epac agonist. A decrease in neurite extension after stimulation with Epac activator is seen in SH-SY5Y cells transfected with shRAPGEF3. (E) The graph presented illustrates the effect of Epac in SH-SY5Y cells neurite extension. The % neurite extensions decrease in SH-SY5Y cells when Epac is silenced by shRAPGEF3. The data shown represent the mean values +/- STD of three independent experiments. Bar=20 µm.

To further elucidate the effects of 8-pCPT-2'-O-Me-cAMP on neurite extension, SH-SY5Y cells were transfected with the Sure Silencing shRAPGEF3 plasmid, designed to specifically knock down the expression of Epac1. The effect of 8-pCPT-2'-O-Me-cAMP on neurite extensions was abolished when Epac 1 was knocked down (Figure 3). Thus, we conclude that Epac-induced signalling mediates the cAMP response that leads to neurite extension in the human neuroblastoma cell line SH-SY5Y.

Epac-induced Alteration of Protein Expression in SH-SY5Y Cells Reflects the Cellular Phenotype

Intrigued by the significant effects of Epac on SH-SY5Y differentiation, we constructed a study to investigate protein expression alterations during cAMP induced differentiation. SILAC in combination with MS is a quantitative proteomics method well suited for comparison between the proteomes of differently treated cell populations (Ong and Mann, 2006). Proteins with 2 or more identified and quantified peptides were grouped and categorized based on the GO biological processes and molecular functional using ProteinCenter and DAVID. Proteins with upregulated expression are over-represented in the GO categories: cell differentiation, cell motility, cell communication and antioxidant activity (Figures 4 and 5).

Upregulated proteins associated with neuronal cell differentiation in Epac stimulated SH-SY5Y cells include: the established neuronal differentiation marker GAP-43, which is present at high level in the neuronal growth cone during differentiation (Brittis et al., 1995); the neuroblast associated differentiation protein (AHNAK), which transports vesicles (enlargosomes) smaller then lysosomes from the proximity of the plasma membrane to neurites during neuronal differentiation (Borgonovo et al., 2002); and the membrane –cytoskeleton linker ankyrin 3 (ANK-3), which plays a key role in cell adhesion at the nodes of Raniver and axonal initial segments (Susuki and Rasband, 2008). Moreover, two other cell adhesion molecules ALCAM (activated leukocyte cell adhesion molecule) and NRCAM (neuronal cell adhesion molecule) are also upregulated. NRCAM is an ankyrin binding protein that has fundamental roles during axonal cone growth and neuron-neuron adhesion (Custer et al., 2003). Together with adhesion molecules we also find proteins involved in

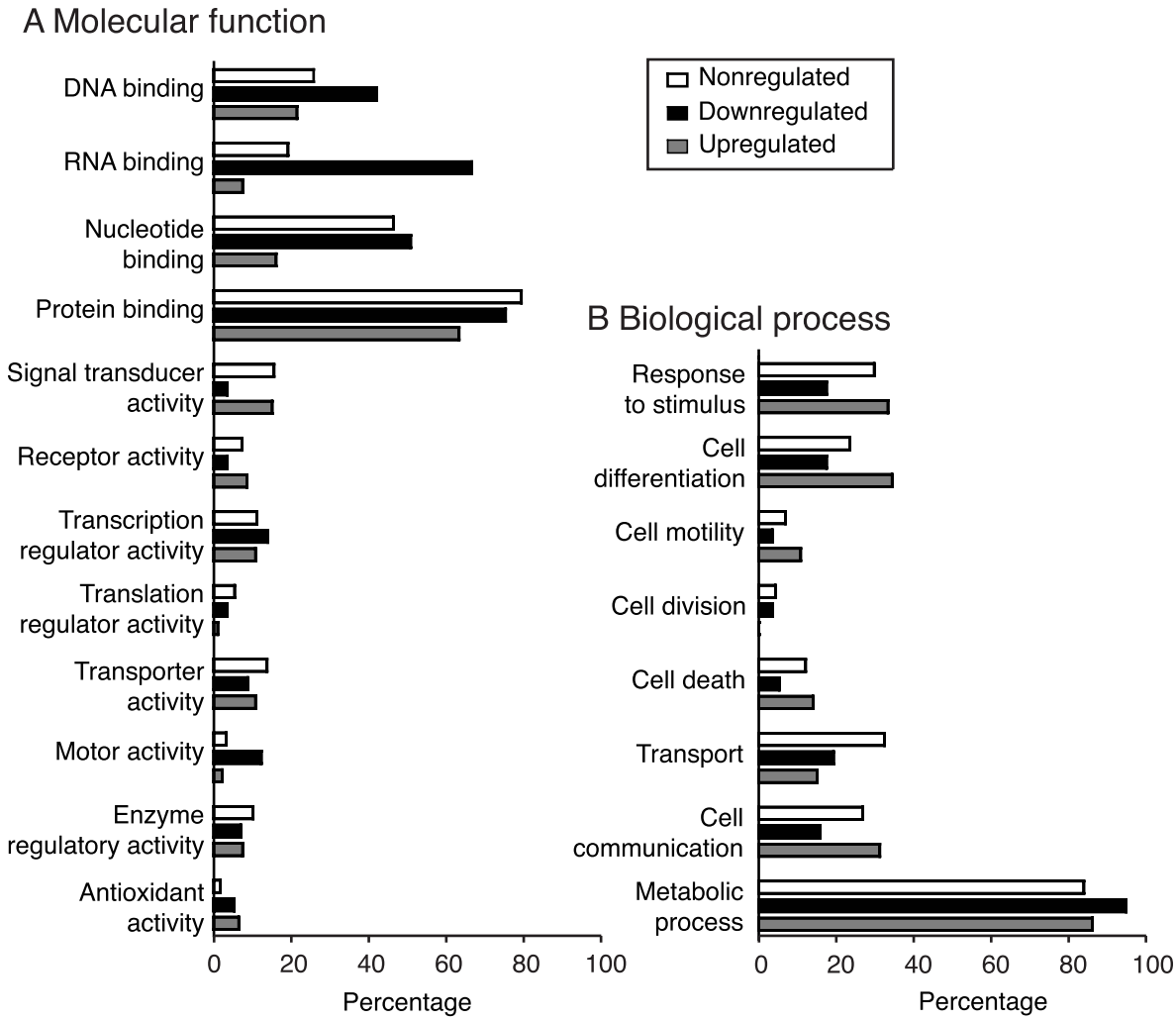

Figure 4: Biological processes and molecular functions affected by Epac agonist stimulation in SH-SY5Y cells
The proteins were analyzed using ProteinCenter software from Proxeon. The bars represent proteins involved in biological processes and molecular functions. A single protein and its isoforms can be present in several groups.

metabolism, such as cytochrome c, to be upregulated. An increase in mitochondrial biogenesis is also found in differentiating P19 mouse embryonal carcinoma cells (Watkins et al., 2008).

The dynamic nature of the growth-cone depends on a range of different cytoskeletal binding proteins, including stathmin. We find stathmin upregulated after 16 hours of Epac stimulation (Figure 5 A). In its unphosphorylated state, stathmin depolymerise microtubuli (Grenningloh et al., 2004) and phosphorylation inhibits these activities, suggesting that stathmin may be affected by extracellular signals.

It has been reported that the at-binding transcription factor 1 (ATBF1) is upregulated in retinoic acid P19 cell differentiation (Hemmi et al., 2006), which is also observed after Epac activation in our study. It is previously suggested that ATFBF1 promotes neuronal differentiation and causes cell cycle arrest (Jung et al., 2005).

Both the constituents of the proteasome and, in addition, the ubiquitin protein are upregulated in our datasets due to Epac activation (Figure 5 and Appendix 1 and 2). Post translational modification by the attachment of ubiquitin seems to have a crucial role in regulating synaptic structure and function (DiAntonio and Hicke, 2004). In terms of axon guidance, proteins such as the E1 ubiquitin-activating enzyme (Appendix 1) and ubiquitin itself have been found in the growth cone. However, the formation of dendrites also depends on ubiquitin. The formation of a neurite to an axon depends on the inactivation of GSK3β by Akt. Akt levels are stable in neurites that develop to axons, but are reduced in a ubiquitin-dependent manner in neurites that develop into dendrites (Segref and Hoppe, 2009).

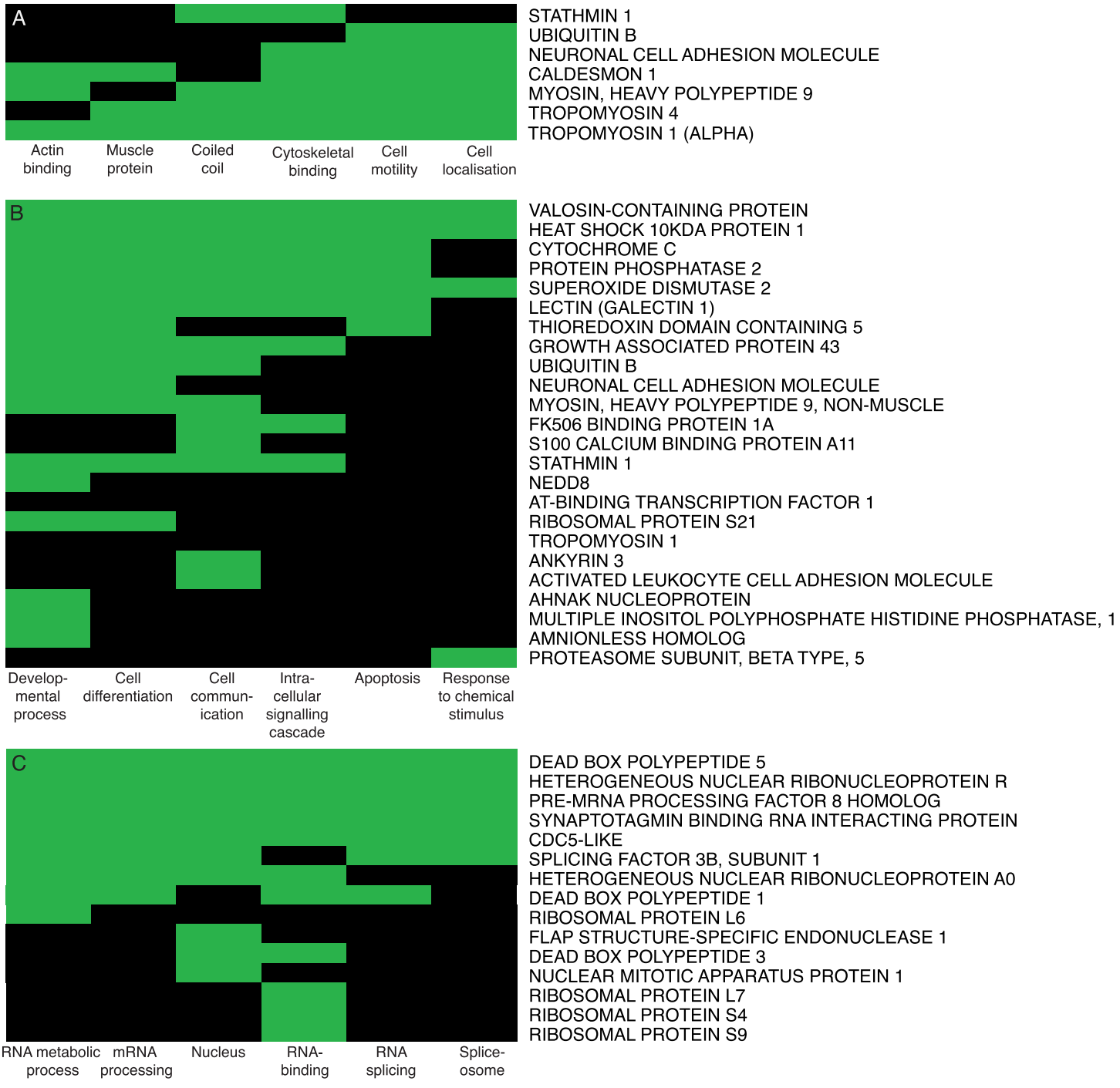

Figure 5: Epac-induced alteration of protein expression in SH-SY5Y cells

VEMS-processed data list for protein quantification (Appendix 2; 1020 proteins including proteins with one quantified peptide) were filtered and analyzed using ProteinCenter. After filtering, 530 proteins (including isoforms) with 2 or more quantified peptides were identified. Upregulated (101) and downregulated (74) proteins were defined as more then 3 fold downregulated and 2 fold upregulated from the normalized average quantitative ratio mean. Using DAVID, single proteins were sorted into GO categories. Only proteins with 2 or more peptides quantified were included in the analysis. The figure shows (A) upregulated proteins involved in cell organization, (B) upregulated proteins involved in cell development, communication and differentiation and (C) downregulated proteins involved in RNA processes and protein synthesis. Green colour = represented in the respective GO category, black = not represented.

Polypyrimidine trackt protein 1 (PTB1) is downregulated in our dataset due to Epac activation (Appendix). The downregulation of PTB1 is needed for neuronal differentiation, but its removal increases neuronal PTB (nPTB) (Boutz et al., 2007). This causes a switch in the alternative splicing which accompanies neuronal differentiation (Boutz et al., 2007). Most of the downregulated proteins in our dataset are involved in RNA processes and protein synthesis (Figure 5 C), including the ribosomal proteins L6, L7, S4 and S9. This is consistent with studies done by others on differentiating neuronal cells (Bevort and Leffers, 2000; Watkins et al., 2008). These results indicate that the overall quantity of new protein required during neuronal differentiation is less than that required for proliferation of the undifferentiated cell population (Watkins et al., 2008).

Conclusion

We here enlarged the proteome of human SH-SY5Y neuroblastoma cells with additionally 72.2%, resulting in 3707 unique proteins. Use of SH-SY5Y Epac knock down cells demonstrates that Epac 1 induces cytoskeleton rearrangement and neurite outgrowth. Cell adhesion proteins, including neuronal cell adhesion molecules and activated leukocyte cell adhesion molecules, and cytoskeletal binding proteins such as stathmin, ankyrin, galectin and myosin are upregulated quantitatively after Epac activation, whereas proteins involved in RNA regulation are downregulated.

The neuronal differential marker protein Gap43 is found upregulated after Epac stimulation. Hereby we conclude that Epac activation induces severe alterations to the proteome of SH-SY5Y cells, many of which favour differentiation towards a neuronal phenotype.

Acknowledgements

We thank Nina Lied Larsen for excellent technical help. This work was supported by the Norwegian Research Council. All experiments were performed at the Proteomic Unit (FUGE Norwegian Research Council) and the Molecular imaging center (FUGE Norwegian Research Council) at the University of Bergen.

References

1. Bevort M, Leffers H (2000) Down regulation of ribosomal protein mRNAs during neuronal differentiation of human NTERA2 cells. Differentiation 66: 81-92. » CrossRef » Pubmed » Google Scholar

2. Biedler JL, Helson L, Spengler BA (1973) Morphology and growth, tumorigenicity, and cytogenetics of human neuroblastoma cells in continuous culture. Cancer Res 33: 2643-2652. » CrossRef » Pubmed » Google Scholar

3. Borgonovo B, Cocucci E, Racchetti G, Podini P, Bachi A, et al. (2002) Regulated exocytosis: a novel, widely expressed system. Nat Cell Biol 4: 955-962. » CrossRef » Pubmed » Google Scholar

4. Bos JL (2006) Epac proteins: multi-purpose cAMP targets. Trends Biochem Sci 31: 680-686. » CrossRef » Pubmed » Google Scholar

5. Boutz PL, Stoilov P, Li Q, Lin CH, Chawla G, et al. (2007) A post-transcriptional regulatory switch in polypyrimidine tract-binding proteins reprograms alternative splicing in developing neurons. Genes Dev 21: 1636-1652. » CrossRef » Pubmed » Google Scholar

6. Bradford MM (1976) A rapid and sensitive method for the quantitation of microgram quantities of protein utilizing the principle of protein-dye binding. Anal Biochem 72: 248-254. » CrossRef » Pubmed » Google Scholar

7. Brittis PA, Meiri K, Dent E, Silver J (1995) The earliest patterns of neuronal differentiation and migration in the mammalian central nervous system. Exp Neurol 134: 1-12. » CrossRef » Pubmed » Google Scholar

8. Chen Y, Takita J, Choi YL, Kato M, Ohira M, et al. (2008) Oncogenic mutations of ALK kinase in neuroblastoma. Nature 455: 971-974. » CrossRef » Pubmed » Google Scholar

9. Christensen AE, Selheim F, de Rooij J, Dremier S, Schwede F, et al. (2003) cAMP analog mapping of Epac1 and cAMP kinase. Discriminating analogs demonstrate that Epac and cAMP kinase act synergistically to promote PC-12 cell neurite extension. J Biol Chem 278: 35394-35402. » CrossRef » Pubmed » Google Scholar

10. Custer AW, Kazarinova-Noyes K, Sakurai T, Xu X, Simon W, et al. (2003) The role of the ankyrin-binding protein NrCAM in node of Ranvier formation. J Neurosci 23: 10032-10039. » CrossRef » Pubmed » Google Scholar

11. De Rooij J, Zwartkruis FJ, Verheijen MH, Cool RH, Nijman SM, et al. (1998) Epac is a Rap1 guanine-nucleotide-exchange factor directly activated by cyclic AMP. Nature 396: 474-477. » CrossRef » Pubmed » Google Scholar

12. De Rooij J, Rehmann H, van Triest M, Cool RH, Wittinghofer A, et al. (2000) Mechanism of regulation of the Epac family of cAMP-dependent RapGEFs. J Biol Chem 275: 20829-20836. » CrossRef » Pubmed » Google Scholar

13. Dennis G Jr, Sherman BT, Hosack DA, Yang J, Gao W, et al. (2003) DAVID: Database for Annotation,

Visualization, and Integrated Discovery. Genome Biol 4: P3. » Pubmed » Google Scholar

14. DiAntonio A, Hicke L (2004) Ubiquitin-dependent regulation of the synapse. Annu Rev Neurosci 27: 223-246. » CrossRef » Pubmed » Google Scholar

15. Edsjo A, Holmquist L, Pahlman S (2007) Neuroblastoma as an experimental model for neuronal differentiation and hypoxia-induced tumor cell dedifferentiation. Semin Cancer Biol 17: 248-256. » CrossRef » Pubmed » Google Scholar

16. George RE, Sanda T, Hanna M, Frohling S, Luther W 2nd, et al. (2008) Activating mutations in ALK provide a therapeutic target in neuroblastoma. Nature 455: 975-978. » CrossRef » Pubmed » Google Scholar

17. Gilany K, Van Elzen R, Mous K, Coen E, Van Dongen W, et al. (2008) The proteome of the human neuroblastoma cell line SH-SY5Y: an enlarged proteome. Biochim Biophys Acta 1784: 983-985. » CrossRef » Pubmed » Google Scholar

18. Grenningloh G, Soehrman S, Bondallaz P, Ruchti E, Cadas H (2004) Role of the microtubule destabilizing proteins SCG10 and stathmin in neuronal growth. J Neurobiol 58: 60-69. » CrossRef » Pubmed » Google Scholar

19. Hedborg F, Bjelfman C, Sparen P, Sandstedt B, Pahlman S (1995) Biochemical evidence for a mature phenotype in morphologically poorly differentiated neuroblastomas with a favourable outcome. Eur J Cancer 31A: 435-443. » CrossRef » Pubmed » Google Scholar

20. Hemmi K, Ma D, Miura Y, Kawaguchi M, Sasahara M, et al. (2006) A homeodomain-zinc finger protein, ZFHX4, is expressed in neuronal differentiation manner and suppressed in muscle differentiation manner. Biol Pharm Bull 29: 1830-1835. » Pubmed » Google Scholar

21. Holz GG, Chepurny OG, Schwede F (2008) Epac-selective cAMP analogs: new tools with which to evaluate the signal transduction properties of cAMP-regulated guanine nucleotide exchange factors. Cell Signal 20: 10-20. » CrossRef » Pubmed » Google Scholar

22. Hosack DA, Dennis G Jr, Sherman BT, Lane HC, Lempicki RA (2003) Identifying biological themes within lists of genes with EASE. Genome Biol 4: R70. » Pubmed » Google Scholar

23. Janoueix-Lerosey I, Lequin D, Brugieres L, Ribeiro A, de Pontual L, et al. (2008) Somatic and germline activating mutations of the ALK kinase receptor in neuroblastoma. Nature 455: 967-970. » CrossRef » Pubmed » Google Scholar

24. Jung CG, Kim HJ, Kawaguchi M, Khanna KK, Hida H, et al. (2005) Homeotic factor ATBF1 induces the cell cycle arrest associated with neuronal differentiation. Development 132: 5137-5145. » CrossRef » Pubmed » Google Scholar

25. Kawasaki H, Springett GM, Mochizuki N, Toki S, Nakaya M, et al. (1998) A family of cAMP-binding proteins that directly activate Rap1. Science 282: 2275-2279. » CrossRef » Pubmed » Google Scholar

26. Kersey PJ, Duarte J, Williams A, Karavidopoulou Y, Birney E, et al. (2004) The International Protein Index: an integrated database for proteomics experiments. Proteomics 4: 1985-1988. » Pubmed » Google Scholar

27. Kiermayer S, Biondi RM, Imig J, Plotz G, Haupenthal J, et al. (2005) Epac activation converts cAMP from a proliferative into a differentiation signal in PC12 cells. Mol Biol Cell 16: 5639-5648. » CrossRef » Pubmed » Google Scholar

28. Lund R, Leth-Larsen R, Jensen ON, Ditzel HJ (2009) Efficient Isolation and Quantitative Proteomic Analysis of Cancer Cell Plasma Membrane Proteins for Identification of Metastasis-Associated Cell Surface Markers. J Proteome Res. » CrossRef » Pubmed » Google Scholar

29. Matthiesen R, Bunkenborg J, Stensballe A, Jensen ON, Welinder KG, et al. (2004) Database-independent, database-dependent, and extended interpretation of peptide mass spectra in VEMS V2.0. Proteomics 4: 2583-2593. » CrossRef » Pubmed » Google Scholar

30. Matthiesen R, Trelle MB, Hojrup P, Bunkenborg J, Jensen ON (2005) VEMS 3.0: algorithms and computational tools for tandem mass spectrometry based identification of post-translational modifications in proteins. J Proteome Res 4: 2338-2347. » CrossRef » Pubmed » Google Scholar

31. Monaghan TK, Mackenzie CJ, Plevin R, Lutz EM (2008) PACAP-38 induces neuronal differentiation of human SH-SY5Y neuroblastoma cells via cAMP-mediated activation of ERK and p38 MAP kinases. J Neurochem 104: 74-88. » CrossRef » Pubmed » Google Scholar

32. Mosse YP, Laudenslager M, Longo L, Cole KA, Wood A, et al. (2008) Identification of ALK as a major familial neuroblastoma predisposition gene. Nature 455: 930-935. » CrossRef » Pubmed » Google Scholar

33. Ong SE, Mann M (2006) A practical recipe for stable isotope labeling by amino acids in cell culture (SILAC). Nat Protoc 1: 2650-2660. » CrossRef » Pubmed » Google Scholar

34. Oveland E, Gjertsen BT, Wergeland L, Selheim F, Fladmark KE, et al. (2009) Ligand-induced Flt3-downregulation modulates cell death associated proteins and enhances chemosensitivity to idarubicin in THP-1 acute myeloid leukemia cells. Leuk Res 33: 276-287. » CrossRef » Pubmed » Google Scholar

35. Pahlman S, Hoehner JC, Nanberg E, Hedborg F, Fagerstrom S, et al. (1995) Differentiation and survival influences of growth factors in human neuroblastoma. Eur J Cancer 31A: 453-458. » CrossRef » Pubmed » Google Scholar

36. Ross RA, Spengler BA, Biedler JL (1983) Coordinate morphological and biochemical interconversion of human neuroblastoma cells. J Natl Cancer Inst 71: 741-747. » CrossRef » Pubmed » Google Scholar

37. Schaeffer V, Patte-Mensah C, Eckert A, Mensah-Nyagan AG (2008) Selective regulation of neurosteroid biosynthesis in human neuroblastoma cells under hydrogen peroxide-induced oxidative stress condition. Neuroscience 151: 758-770. » Pubmed

38. Segref A, Hoppe T (2009) Think locally: control of ubiquitin-dependent protein degradation in neurons. EMBO Rep 10: 44-50. » CrossRef » Pubmed » Google Scholar

39. Shevchenko A, Tomas H, Havlis J, Olsen JV, Mann M (2006) In-gel digestion for mass spectrometric characterization of proteins and proteomes. Nat Protoc 1: 2856-2860. » CrossRef » Pubmed » Google Scholar

40. Shi GX, Rehmann H, Andres DA (2006) A novel cyclic AMP-dependent Epac-Rit signaling pathway contributes to PACAP38-mediated neuronal differentiation. Mol Cell Biol 26: 9136-9147. » CrossRef » Pubmed » Google Scholar

41. Susuki K, Rasband MN (2008) Spectrin and ankyrin-based cytoskeletons at polarized domains in myelinated axons. Exp Biol Med 233: 394-400. » CrossRef » Pubmed » Google Scholar

42. Watkins J, Basu S, Bogenhagen DF (2008) A quantitative proteomic analysis of mitochondrial participation in p19 cell neuronal differentiation. J Proteome Res 7: 328-338. » CrossRef » Pubmed » Google Scholar

43. Zufall F, Shepherd GM, Barnstable CJ (1997) Cyclic nucleotide gated channels as regulators of CNS development and plasticity. Curr Opin Neurobiol 7: 404-412. » CrossRef » Pubmed » Google Scholar